Received: 1 September 2016 | Revised: XXXX | Accepted: 19 December 2016

DOI: 10.1002/asna.201713294

ORIGINAL ARTICLE

Astronomische Nachrichten

The cataclysmic variable AE Aquarii: B–V color of the flares†

R. K. Zamanov[1]*† | G. Y. Latev[1] | S. Boeva[1] | S. Ibryamov[2] | G. B. Nikolov[1] | K. A. Stoyanov[1]

[1]Institute of Astronomy and National Astronomical Observatory, Bulgarian Academy of Sciences, Sofia, Bulgaria

[2]Department of Physics, Konstantin Preslavsky University of Shumen, Shumen, Bulgaria

***Correspondence**

R. K. Zamanov, Institute of Astronomy and National Astronomical Observatory, Bulgarian Academy of Sciences, Tsarigradsko shose 72, BG-1784 Sofia, Bulgaria.

Email: rkz@astro.bas.bg

†Observations from National Astronomical Observatory Rozhen and AO Belogradchick, Bulgaria.

We report simultaneous observations of the flaring behavior of the cataclysmic variable star AE Aquarii (AE Aqr). The observations are in Johnson B and V bands. The color–magnitude diagrams (B–V vs. V and B–V vs. B) show that the star becomes more blue as it becomes brighter. In our model, AE Aqr's behavior can be explained with flares (fireballs) with $0.03 \leq B\text{–}V \leq 0.30$, and temperature in the interval $8000 \leq T \leq 12000$.

KEYWORDS

Stars: novae, cataclysmic variables – Accretion, accretion disks – white dwarfs – Stars: individual: AE Aqr

1 | INTRODUCTION

AE Aquarii (AE Aqr) is a bright ($V \sim 11$ mag.), unusual, cataclysmic variable (CV), displaying strong flaring activity (e.g., Chincarini & Walker 1974). Its binary nature was discovered by Joy (1954). In the system, a spotted K-type dwarf (K0-K4 IV/V star) transfers material through the inner Lagrangian point L_1 toward a magnetic white dwarf (Hill et al. 2016; Skidmore et al. 2003). It has a relatively long (for a CV) orbital period of 9.88 hr (e.g., Casares et al. 1996) and a very short spin period of the white dwarf of only 33 s, detected in the optical and X-ray bands (Patterson et al. 1980). To appear in such a state, AE Aqr should be a former supersoft X-ray binary, in which the mass transfer rate in the recent past ($\approx 10^7$ year) must have been much higher than its current value (Schenker et al. 2002).

The high-dispersion, time-resolved absorption line spectroscopy by Echevarría et al. (2008) gives the binary parameters as follows: white dwarf mass $M_{WD} = 0.63 \pm 0.05\ M_\odot$; secondary mass $M_2 = 0.37 \pm 0.04\ M_\odot$; binary separation $a = 2.33 \pm 0.02\ R_\odot$; and inclination $i \approx 70°$.

The observations obtained to date contain no clear evidence for an accretion disk. Given the lack of such evidence, speedy magnetic propeller (Eracleous & Horne 1996; Wynn et al. 1997) and ejector (Ikhsanov & Beskrovnaya 2012; Ikhsanov et al. 2004) are supposed to operate in this star. Hydrodynamic calculations hint that the field does not hinder the formation of a transient disk (ring) surrounding the magnetosphere (Isakova et al. 2016). AE Aqr also exhibits radio and millimeter synchrotron emission (e.g., Bastian et al. 1988; Bookbinder & Lamb 1987). *XMM-Newton* observations demonstrate that the plasma cannot be a product of mass accretion onto the white dwarf (Itoh et al. 2006). The non-detection of very high energy (TeV) γ-rays in MAGIC observations (Aleksić et al. 2014) probably points that the white dwarf is not acting as an ejector and, in our point of view, the propeller model is the better one.

In the optical bands, AE Aqr exhibits atypical flickering consisting of large optical flares with amplitude ≤ 1 magnitude in the Johnson V band. The flares are visible about one-third of the time and have typical rise times of $200 - -400$ s (van Paradijs et al. 1989; Zamanov et al. 2012). The flares are also visible in the X-ray (Mauche et al. 2012) and submillimeter wavelengths (Torkelsson 2013).

Here we explore the behavior of AE Aqr in the optical B and V bands, construct the color–magnitude diagram, and estimate the B–V color of the flares and temperature of the fireballs.

2 | OBSERVATIONS

The observations of the short-term variability of AE Aqr were obtained with four telescopes: the 2.0 m RCC telescope, the 50/70 cm Schmidt telescope, the 60 cm telescope of the Bulgarian National Astronomical Observatory Rozhen, and the 60 cm telescope of the Belogradchick

TABLE 1 Simultaneous observations of AE Aqr in B and V bands

	D	B			V			
Date	**(min)**	**Telescope**	**Exp. time (s)**	N_B	**Telescope**	**Exp. time (s)**	N_V	N_{B-V}
20100813	162	50/70Sch	60	137	2.0m	5, 10	463	110
20100814	299	50/70Sch	60, 120	246	2.0m	10	1013	228
20100816	353	60Roz	60, 90	75	60Roz	60	68	60
20110831	180	50/70Sch	30	270	2.0m	5	1087	258
20110924	166	60Bel	20	160	60Bel	10	160	160
20110927	164	60Bel	15	200	60Bel	10	200	200
20110928	123	60Bel	15	150	60Bel	10	150	150
20120814	189	50/70Sch	15	442	2.0m,60R	5, 10	395	327
20120815	167	60Roz	30	158	50/70Sch	10	75	60
20120816	121	50/70Sch	15	380	2.0m	3, 10	282	282
20120908	107	50/70Sch	20	190	60Roz	10	347	167
20130915	221	50/70Sch	10	325	50/70Sch	5	325	325

The columns give date of observation (in format YYYYMMDD), duration of the run (in minutes), telescope, exposure times of the CCD frames, and number of data points in the run for B and V bands. The last column gives the number of data points over which the *B–V* color was calculated.

AE Aquarii = AE Aqr; CCD = charge-coupled device

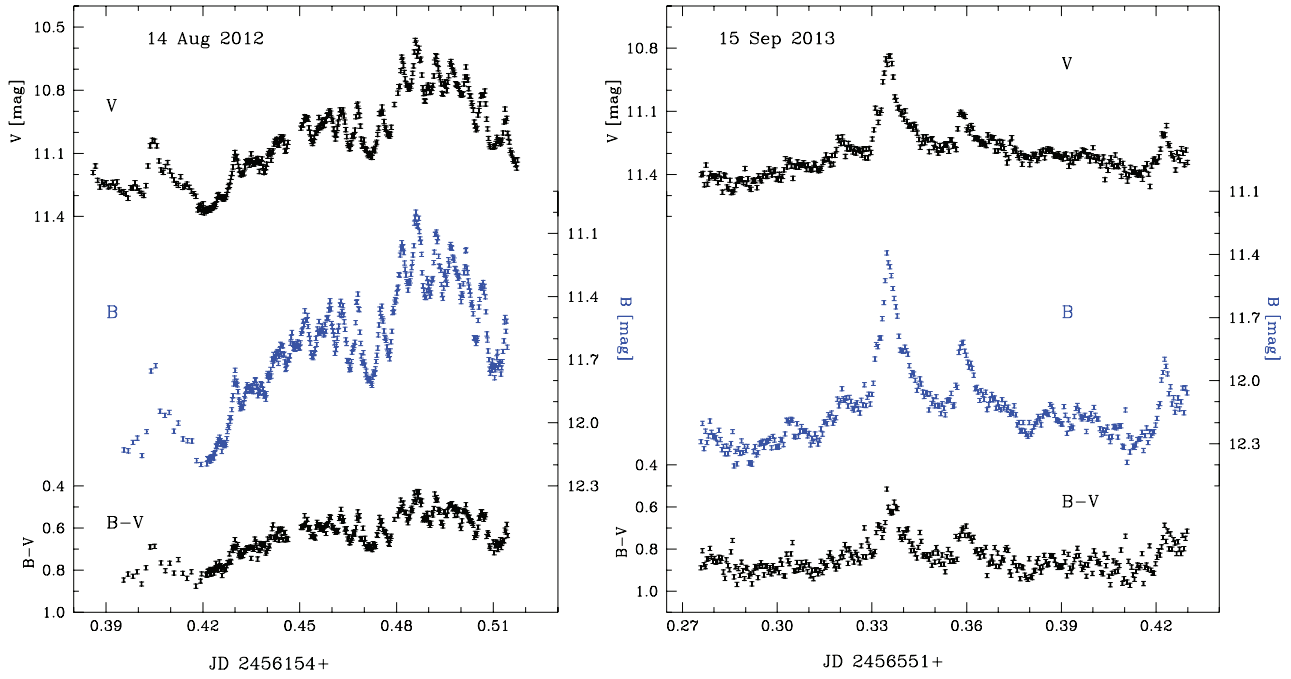

FIGURE 1 Simultaneous observations of AE Aquarii in B and V bands obtained on August 14, 2012, and September 15, 2013. The calculated *B–V* color index is also plotted. When the brightness of the star increases, the *B–V* index becomes more blue

Astronomical Observatory. All these telescopes are equipped with charge-coupled device (CCD) cameras. All the CCD images were bias-subtracted and flat-fielded, and standard aperture photometry was performed. Data reduction and aperture photometry were carried out with IRAF and checked with alternative software packages. The typical accuracy of the photometry was 0.005–0.010 mag. The journal of observations is given in Table 1. The first four dates were partly analyzed in Zamanov et al. (2012). The others are new observations. Two examples of our observations are presented in Figure 1.

3 | LIGHT CURVES IN THE B AND V BANDS

Stochastic light variations on timescales of a few minutes (flickering) with amplitude of a few×0.1 magnitudes are a type of variability observed in the three main classes of binaries that contain white dwarfs accreting material from a companion mass-donor star: CVs, supersoft X-ray binaries, and symbiotic stars (e.g., Sokoloski 2003). Stochastic light variations are observed not only in accreting white dwarfs but also in accreting black holes and neutron stars (e.g., Belloni & Stella 2014; Scaringi 2015).

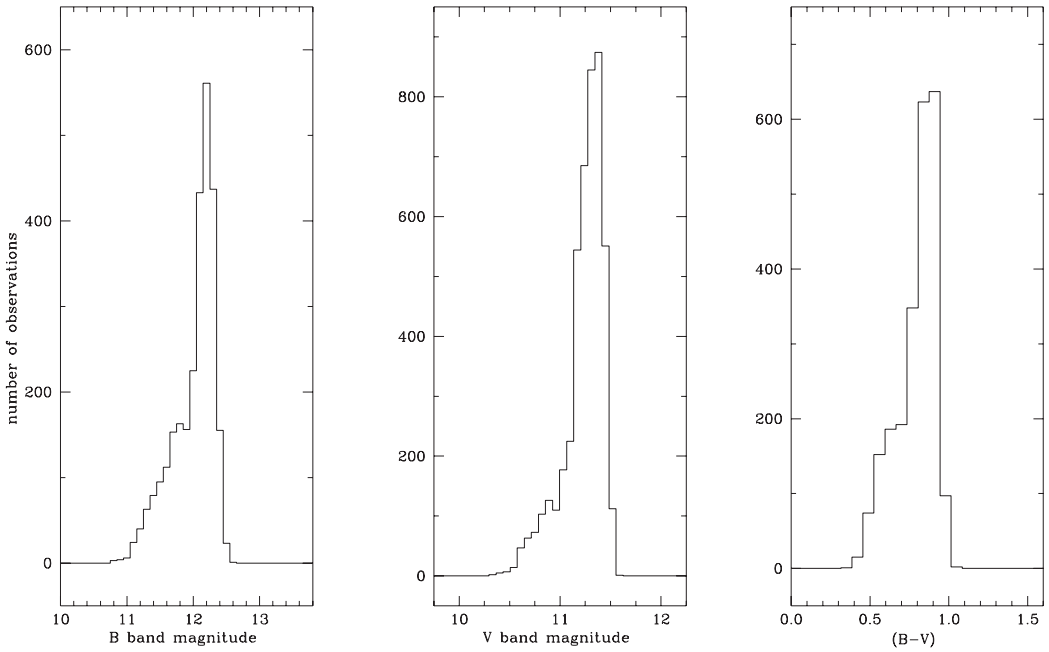

FIGURE 2 Histograms representing the distribution of B and V band magnitudes and B–V color. V, B, and B–V were calculated for a total number of 2,473 data points

The flickering of AE Aqr was first detected by Henize (1949). The five-color optical photometry using the Walraven system performed in 1984 and 1985 was analyzed by van Paradijs et al. (1989). In Figure 1, we have plotted the variability of AE Aqr in the B and V bands. The calculated color index is also plotted. All data were drawn on identical scales; in this way, 0.1 magnitude has the same size on all Y-axes.

Histograms representing the distribution of B and V band magnitudes and B–V color are plotted in Figure 2. The B magnitude is measured for $N_{pts} = 2733$. The values are in the interval $10.767 \leq B \leq 12.565$, with an average value of $\overline{B} = 12.006$, standard deviation of the mean $\sigma_B = 0.320$, and median value $\langle B \rangle = 12.112$. The V magnitude is measured for $N_{pts} = 4564$. The values are in the interval $10.355 \leq V \leq 11.563$, with average value $\overline{V} = 11.235$, $\sigma_V = 0.199$, and median value $\langle V \rangle = 11.288$. The histograms of the B and V band magnitudes have a well-defined peak and an extended tail to the higher brightness side. The peaks of the distributions are at $V = 11.35 \pm 0.03$ and at $B = 12.22 \pm 0.03$ for the V and the B band, respectively. B–V is measured for $N_{pts} = 2327$ data points. The values are at the interval $0.354 \leq B$–$V \leq 1.037$, with the average value $\overline{B-V} = 0.794$, $\sigma_{B-V} = 0.126$, and median value $\langle B$–$V \rangle = 0.829$.

The histogram of B–V color has a well-defined peak at B–$V = 0.88 \pm 0.03$ and an extended tail toward the blue. The tails in all three histograms plotted (Figure 2) are due to the appearance of the flares in the light curve.

4 | COLOR–MAGNITUDE DIAGRAM

In Figure 3, we have shown the relation between the brightness of the star in the B and V bands and its B–V color. It is seen that the star becomes more blue when it brightens and more red when it fades, indicating that the flares change the color of the system.

Pearson et al. (2003) have suggested that the flares of AE Aqr are due to the ejection and expansion of isothermal fireballs. Using their improved model (Pearson et al. 2005), Zamanov et al. (2012) have estimated the fireballs temperatures of 10000–25000 K, masses of $(7\text{–}90) \times 10^{19}$ g, and sizes of $(3\text{–}7) \times 10^9$ cm (using a distance of $d = 86$ pc). These values refer to the peak of the flares observed in the UBVRI bands. Here we use $E(B$–$V)$=0 (La Dous 1991), and construct the color–magnitude diagrams. These diagrams should contain information about the temperature of the flares. We model the behavior of AE Aqr in the following way:

- The peak of the V band histogram corresponds to $V = 11.35$. The peak of the B band histogram corresponds to $B = 12.22$. We adopt these values as the basic levels.
- To this level we add an additional source (fireball) with constant B–V. We vary the brightness of this additional source from 15.0 to 10.95 mag. in V.
- Because the stellar magnitude scale is logarithmic, during the calculations we convert the magnitudes into fluxes using the Bessell (1979) calibration of a zero-magnitude star. After this, we reconvert the fluxes into magnitudes.
- We repeat this procedure with a different B–V color of the fireball. We achieved the best agreement with B–$V = 0.19$ of the fireball.

The basic level is as follows:

$$F_{V0} = 3.610 \times 10^{-9} \times 10^{-11.35/2.5} \quad \text{erg cm}^{-2}\ \text{s}^{-1}\ \text{Å}^{-1}, \quad (1)$$

$$F_{B0} = 6.601 \times 10^{-9} \times 10^{-12.22/2.5} \quad \text{erg cm}^{-2}\ \text{s}^{-1}\ \text{Å}^{-1}, \quad (2)$$

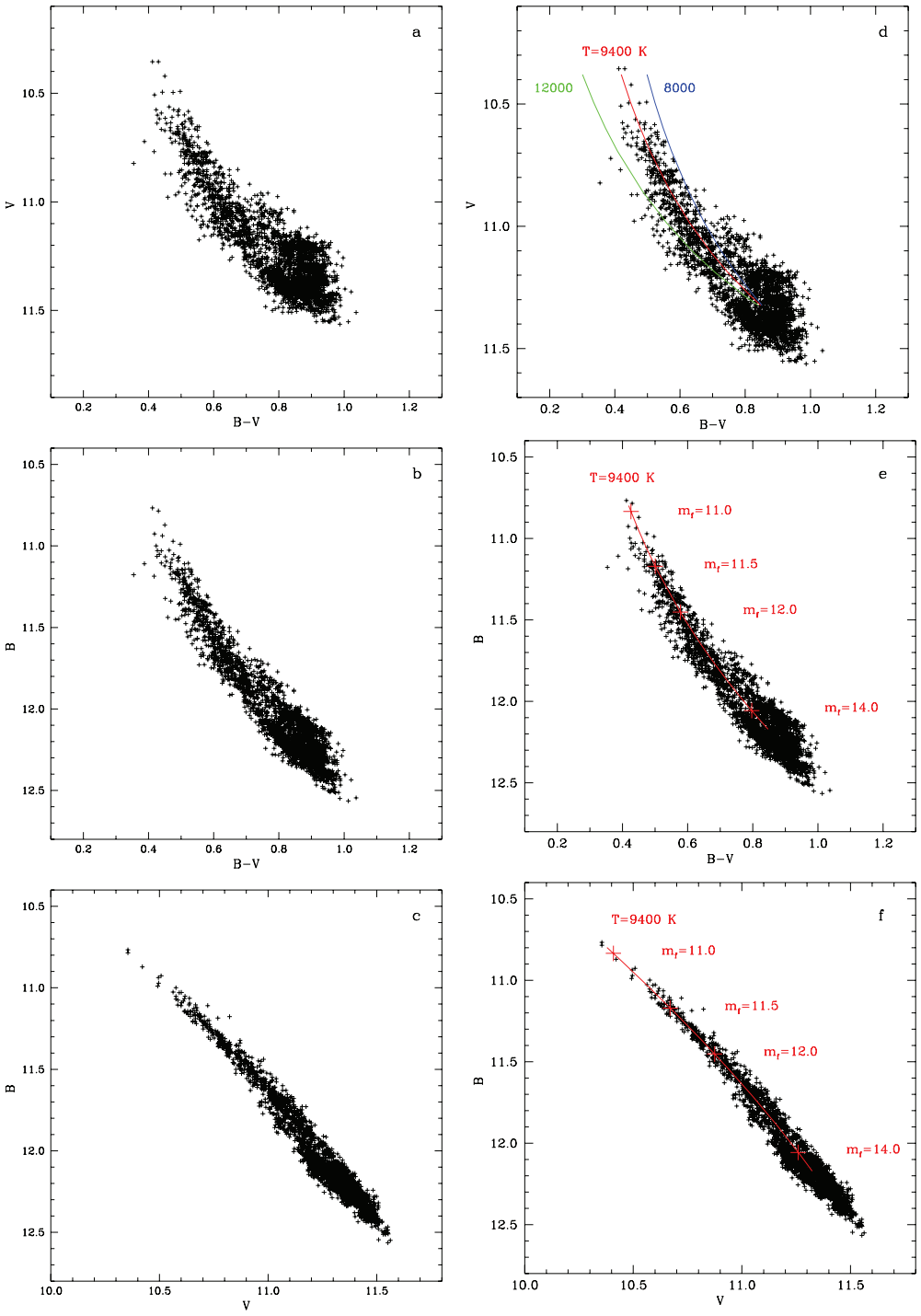

FIGURE 3 Color–magnitude diagrams of the peculiar cataclysmic variable AE Aqr. (Left panels): (a) V versus B–V. (b) B versus B–V, (c) B versus V. On the right panels, the models are over-plotted

where F_{V0} and F_{B0} are the fluxes corresponding to the peak of the histograms in the V and B band, respectively. The emission of the fireball is

$$F_{Vf} = 3.610 \times 10^{-9} \times 10^{-m_f/2.5} \quad \mathrm{erg\ cm^{-2}\ s^{-1}\ \AA^{-1}} \tag{3}$$

$$F_{Bf} = 6.601 \times 10^{-9} \times 10^{-(m_f+c_f)/2.5} \quad \mathrm{erg\ cm^{-2}\ s^{-1}\ \AA^{-1}}, \tag{4}$$

where m_f is the V-band magnitude of the fireball, c_f is its B–V color. F_{Vf} and F_{Bf} are the fluxes of the ball emitted in the V and B band, respectively. The brightness of the system (F_V and F_B) is the sum of the fluxes of the basic level and the fireball:

$$F_V = F_{V0} + F_{Vf} \tag{5}$$

$$F_B = F_{B0} + F_{Bf} \tag{6}$$

$$m_V = -2.5\ \log(F_V/(3.610 \times 10^{-9})) \tag{7}$$

$$m_B = -2.5\ \log(F_B/(6.601 \times 10^{-9})) \tag{8}$$

where m_V and m_B are the brightness of the system in magnitudes for the V and B band, respectively. In Figure 3d we plot

with green, red, and blue color three lines corresponding to the B–V color of the fireball $c_f = 0.03$, 0.19, and 0.30. These B–V colors correspond to black body temperatures 12000, 9400, and 8000 K, respectively. The model with $c_f = 0.19$ produces good agreement with the observations in the three panels: V versus B–V (Figure 3d), B versus B–V (Figure 3e), and B versus V (Figure 3f). In Figure 3e and f, we have marked with red crosses four positions corresponding to V brightness values of the fireball $m_f = 11.0,\ 11.5,\ 12.0,\ 14.0$.

The largest flares of AE Aqr correspond to an additional source with $V \approx 10.95$ mag., which is the brightness of the most luminous flares (fireballs) in our dataset. Comparing this value with the peak of the histogram, we derive that in the V band the strongest flares emit 1.4 times as much energy as the non-flaring components of AE Aqr (in the B band they emit 2.2 times). The values are similar but higher than the value 1.5× for the strongest flares observed in the B band in 1983 (Bruch 1991).

5 | DISCUSSION

AE Aqr is a highly variable object exhibiting flaring behavior in the optical (Chincarini & Walker 1981), radio (Bastian et al. 1988), ultraviolet (Eracleous & Horne 1996), and X-ray (Choi & Dotani 2006) regions. Five-color (Walraven system) observations of the CV AE Aqr were made in 1984 and 1985 (van Paradijs et al. 1989). The optical flux emitted in the flares is about 3× the quiescent accretion flux. There seems to be a slight phase dependence of the activity—while flares can definitely occur at any phase, the probability for very strong variations is higher in the first half of the orbital cycle than in the second half (Bruch & Grutter 1997).

Different mechanisms have been proposed to explain the flares of AE Aqr:

(1) The flares are due to an accretion instability that occurs within a few white dwarf radii, perhaps as a result of the magnetospheric gating of the inflowing matter at the inner edge of the accretion disk (van Paradijs et al. 1989).

(2) They are due to the blobs (fireballs) launched from the magnetosphere (Pearson et al. 2002; Wynn et al. 1997).

In the context of the fragmented accretion flow/magnetic propeller scenario, we assume that the flares represent the excitation of gaseous blobs upon encounter with the propeller and their subsequent radiative cooling as they are expelled from the system. The gas stream emerging from L_1 encounters a rapidly spinning magnetosphere of the white dwarf. The rapid spin causes the stream material to be dragged toward co-rotation with the magnetosphere. As it occurs outside the co-rotation radius, the magnetosphere velocity of the material accelerates beyond the escape velocity (Wynn et al. 1997).

The color versus magnitude diagrams (Figure 3) indicate that the balls have temperatures in the range $8000 \lesssim T_f \lesssim 12000$ K and the V band magnitude $14.0 \lesssim m_f \lesssim 11.0$. Our result point to the fact that all the fireballs have similar temperature of $\sim$ 9400 K. Taking into account the observational errors and errors in the fit, we estimate the average temperature of the fireballs as 9400 ± 600 K. There is no tendency (at least in our data) for the brighter flares to have a higher or lower temperature. This is in agreement with the suppositions that the flares are isothermal (Pearson et al. 2003). This temperature is similar to that of the flickering source of the recurrent nova RS Oph $T = 9500 \pm 500$ K (Zamanov et al. 2010).

6 | CONCLUSION

We performed 37.5 hr of simultaneous observations in Johnson B and V bands of the CV AE Aqr. On the basis of these observations, the B–V color is calculated for 2327 observational points. The color versus magnitude diagrams show that the star becomes more blue as it becomes brighter. We modeled the brightness (B and V band) and B–V color changes, assuming an additional source of energy (blobs). The model indicates that the blobs (flares) have on average B–V of 0.19, which corresponds to an average temperature of the fireballs of 9400 ± 600 K.

A related question is whether the color versus magnitudes diagrams and model discussed here are relevant to other cataclysmic and symbiotic flickering stars.

ACKNOWLEDGMENTS

This work was supported by the Program for Career Development of Young Scientists, Bulgarian Academy of Sciences.

REFERENCES

Aleksić, J., Ansoldi, S., Antonelli, L. A., et al. 2014, *Astron. Astrophys.*, *568*, A109.
Bastian, T. S., Dulk, G. A., & Chanmugam, G. 1988, *Astrophys. J.*, *324*, 431.
Belloni, T. M., & Stella, L. 2014, *Space Sci. Rev.*, *183*, 43.
Bessell, M. S. 1979, *Publ. Astron. Soc. Pacific*, *91*, 589.
Bookbinder, J. A., & Lamb, D. Q. 1987, *Astrophys. J.*, *323*, L131.
Bruch, A. 1991, *Astron. Astrophys.*, *251*, 59.
Bruch, A., & Grutter, M. 1997, *Acta Astron.*, *47*, 307.
Casares, J., Mouchet, M., Martinez-Pais, I. G., & Harlaftis, E. T. 1996, *Mon. Not. R. Astron. Soc.*, *282*, 182.
Chincarini, G., & Walker, M. F. 1974, Electrography and astronomical applications. Proc. Conf. (A75-23926 09–89), University of Texas, Austin, 249
Chincarini, G., & Walker, M. F. 1981, *Astron. Astrophys.*, *104*, 24.
Choi, C.-S., & Dotani, T. 2006, *Astrophys. J.*, *646*, 1149.
Echevarría, J., Smith, R. C., Costero, R., Zharikov, S., & Michel, R. 2008, *Mon. Not. R. Astron. Soc.*, *387*, 1563.
Eracleous, M., & Horne, K. 1996, *Astrophys. J.*, *471*, 427.
Henize, K. G. 1949, *Astronom. J.*, *54*, 89.
Hill, C. A., Watson, C. A., Steeghs, D., Dhillon, V. S., & Shahbaz, T. 2016, *Mon. Not. R. Astron. Soc.*, *459*, 1858.
Ikhsanov, N. R., & Beskrovnaya, N. G. 2012, *Astron. Rep.*, *56*, 595.
Ikhsanov, N. R., Neustroev, V. V., & Beskrovnaya, N. G. 2004, *Astron. Lett.*, *30*, 675.
Isakova, P. B., Ikhsanov, N. R., Zhilkin, A. G., Bisikalo, D. V., & Beskrovnaya, N. G. 2016, *Astron. Rep.*, *60*, 498.
Itoh, K., Okada, S., Ishida, M., & Kunieda, H. 2006, *Astrophys. J.*, *639*, 397.
Joy, A. H. 1954, *Astronom. J.*, *59*, 326.
La Dous, C. 1991, *Astron. Astrophys.*, *252*, 100.

Mauche, C. W., Abada-Simon, M., Desmurs, J.-F., & etaltext 2012, *Mem. Soc. Astron. Italiana*, *83*, 651.

Patterson, J., Branch, D., Chincarini, G., & Robinson, E. L. 1980, *Astrophys. J.*, *240*, L133.

Pearson, K. J., Horne, K., & Skidmore, W. 2002, The Physics of Cataclysmic Variables and Related Objects, Vol. 261, 163

Pearson, K. J., Horne, K., & Skidmore, W. 2003, *Mon. Not. R. Astron. Soc.*, *338*, 1067.

Pearson, K. J., Horne, K., & Skidmore, W. 2005, *Astrophys. J.*, *619*, 999.

Scaringi, S. 2015, Acta Polytechnica CTU Proc., Vol. 2, 107

Schenker, K., King, A. R., Kolb, U., Wynn, G. A., & Zhang, Z. 2002, *Mon. Not. R. Astron. Soc.*, *337*, 1105.

Skidmore, W., O'Brien, K., Horne, K., & etaltext 2003, *Mon. Not. R. Astron. Soc.*, *338*, 1057.

Sokoloski, J. L. 2003, Symbiotic Stars Probing Stellar Evolution, ASP Conf., Vol. 303, 202

Torkelsson, U. 2013, Feeding Compact Objects: Accretion on All Scales, IAU Symp., Vol. 290, 145

van Paradijs, J., van Amerongen, S., & Kraakman, H. 1989, *Astron. Astrophys. Suppl.*, *79*, 205.

Wynn, G. A., King, A. R., & Horne, K. 1997, *Mon. Not. R. Astron. Soc.*, *286*, 436.

Zamanov, R. K., Boeva, S., Bachev, R., & etaltext 2010, *Mon. Not. R. Astron. Soc.*, *404*, 381.

Zamanov, R. K., Latev, G. Y., Stoyanov, K. A., & etaltext 2012, *Astron. Nachr.*, *333*, 736.

How to cite this article: Zamanov RK, Latev GY, Boeva S, Ibryamov S, Nikolov GB, Stoyanov KA. The cataclysmic variable AE Aquarii: *B–V* color of the flares, *Astron. Nachr./AN*, 2017;00:1–6. https://doi.org/10.1002/asna.201713294